JAERI-M
7545

SLOW NEUTRON RESONANCES IN Tb-159

February 1978

Makio OHKUBO and Yuuki KAWARASAKI

日本原子力研究所
Japan Atomic Energy Research Institute

JAERI-M 7545

Slow Neutron Resonances in Tb-159

Makio OHKUBO and Yuuki KAWARASAKI

Physics Division,

Tokai Research Establishment, JAERI

(Received January 27, 1978)

An experiment of neutron resonances in Tb-159 was carried out using the JAERI linac time-of-flight facility. Transmission and capture measurements were made on terbium samples of two thicknesses, using ^{6}Li-glass scintillators and Moxon-Rae detector at the 47m station of the TOF facility; the neutron flux was monitored with a ^{6}Li-glass transmission type flux monitor. Transmission data were analyzed with an area analyses program up to 1.2 keV, and capture data with Monte= Carlo program CAFIT, to obtain $2g\Gamma_n^o$, Γ and Γ_γ. Spin determinations were also made for large resonances. Between 754 to 1192 eV, 50 new levels were analyzed. The results are as follows; average level spacing $\langle D \rangle = 4.4 \pm 0.4$ eV below 600 eV, s-wave strength function $S_o = (1.55 \pm 0.15)10^{-4}$ for 206 levels below 1.2 keV, and average radiation width $\langle \Gamma_\gamma \rangle = 107 \pm 7$ meV for lower 25 levels. Average capture cross section $\langle \sigma_c \rangle$ were obtained from 50 eV to 30 keV.

Keywords: Slow Neutron Resonance, Terbium-159, EnergyRange-1200eV, EnergyLevels, Resonance Parameters, Level Spacing Strenth Function Average radiation width, Average capture cross section.

JAERI－M 7545

Tb－159における低速中性子共鳴

日本原子力研究所東海研究所物理部

大久保　牧夫・河原崎　雄紀

（1978年1月27日受理）

原研リニアック中性子飛行時間測定装置により，Tb－159の共鳴について実験を行った。二種類の厚さのTb試料について，中性子透過及び捕獲の測定を，47m測定室にある ^{6}Li－glass及びMoxon－Rae検出器を用いて行った。透過率データは面積法により，1.2KeVまで，また捕獲データは，モンテカルロ・プログラムCAFITにより，$2g\Gamma_n^o$，Γ，Γ_γ を得た。大きい共鳴については，スピン決定がなされた。新たに754eV以上，1192eVまでの50本のレベルを解析して，以下の結果を得た。600eV以下で平均レベル間隔$<D>$＝4.4±0.4eV，1.2KeVまでの206本のレベルのS波強度関数So＝（1.55±0.15）10^{-4}，また低い25本のレベルについての平均輻射巾$<\Gamma_\gamma>$＝107±7meV，平均捕獲断面積を50eVから30KeVの間で求めた。

CONTENTS

Slow Neutron Resonances in Tb-159

Makio OHKUBO and Yuuki KAWARASAKI

1. Introduction

Neutron cross sections are one of the basic data for understanding neutron-nucleus interactions, and also important for reactor engineering. Neutron resonance data of a rare earth element Tb-159 were very poor when the present measurement were planned, though some measurements had been made;[1,2,3] the resonance parameters below 113 eV are compiled in reference 4. Recently Derrien et al.[5] reported the results of high resolution transmission measurements up to 753 eV, and Popov et al.[6] up to 580 eV. Level spins up to 311 eV have been determined with pulsed reactor IBR-30 at Dubna, using polarized neutrons and polarized terbium target.[7] Average capture cross sections have been measured by Gibbon et al.[8] from 10 to 180 keV, and by Block et al.[9] from 0.2 to 10 keV using large liquid scintillator. Intermediate structures have been reported by Jain et al.[10] in capture gamma-ray yield ratio for high and low biases for NaI(Tl) gamma ray detector with neutron energies below 1 keV. Mizumoto et al.[11] observed anomalously small gamma ray multiplicity in a few keV neutron energy region.

It is of importance to measure capture cross section as well as total cross sections of this monoisotopic element (Z=65, A=159, 100%) for the unambiguous interpretation in the statistical properties of the levels in the resonance energy region, and also interesting to seek for possible intermediate stuctures or some deviation from a statistical model of the compound nucleus.

In this report the results are described of the transmission and capture measurements on terbium at the 47 m station of the JAERI linac time-of-flight facility, using ^{6}Li-glass scintillators and a Moxon-Rae detector. More than 200 levels up to 1.2 keV were analyzed to obtain E_0, $2g\Gamma_n^0$ and in favourable cases Γ, Γ_γ, and spin J. Average level spacing, strength function, and average capture cross section were obtained.

2. Measurements and Analyses

The JAERI linac time-of-flight spectrometer[12] and the method of analyses are described in the following.

Slow Neutron Resonances in Tb-159

Makio OHKUBO and Yuuki KAWARASAKI

1. Introduction

Neutron cross sections are one of the basic data for understanding neutron-nucleus interactions, and also important for reactor engineering. Neutron resonance data of a rare earth element Tb-159 were very poor when the present measurement were planned, though some measurements had been made;[1,2,3] the resonance parameters below 113 eV are compiled in reference 4. Recently Derrien et al.[5] reported the results of high resolution transmission measurements up to 753 eV, and Popov et al.[6] up to 580 eV. Level spins up to 311 eV have been determined with pulsed reactor IBR-30 at Dubna, using polarized neutrons and polarized terbium target.[7] Average capture cross sections have been measured by Gibbon et al.[8] from 10 to 180 keV, and by Block et al.[9] from 0.2 to 10 keV using large liquid scintillator. Intermediate structures have been reported by Jain et al.[10] in capture gamma-ray yield ratio for high and low biases for NaI(Tl) gamma ray detector with neutron energies below 1 keV. Mizumoto et al.[11] observed anomalously small gamma ray multiplicity in a few keV neutron energy region.

It is of importance to measure capture cross section as well as total cross sections of this monoisotopic element (Z=65, A=159, 100%) for the unambiguous interpretation in the statistical properties of the levels in the resonance energy region, and also interesting to seek for possible intermediate stuctures or some deviation from a statistical model of the compound nucleus.

In this report the results are described of the transmission and capture measurements on terbium at the 47 m station of the JAERI linac time-of-flight facility, using ^{6}Li-glass scintillators and a Moxon-Rae detector. More than 200 levels up to 1.2 keV were analyzed to obtain E_o, $2g\Gamma_n^o$ and in favourable cases Γ, Γ_γ, and spin J. Average level spacing, strength function, and average capture cross section were obtained.

2. Measurements and Analyses

The JAERI linac time-of-flight spectrometer[12] and the method of analyses are described in the following.

(Linac and Target)

The JAERI s-band electron linac consists of 5 accelerating waveguides (two by MITSUBISHI Electric Co. and three by ARCO) each of which is supplied with an RF power from a klystron of maximum 20 MW at 2856MHz. The nominal beam energy is 120 MeV, with maximum beam current 1.8A for 80 nsec pulse in repetition rate 150 pps. Figure 1 shows the TOF spectrometer and the target assembly. The electron beam is conducted straight through a beam duct with a several focusing Q-lens system to a neutron production target in a heavily shielded concrete room. About 2 m before the target, a small bending magnet deflects the beam by 15 cm downward to hit the target where center lines of neutron flight tubes intersect. The neutron target consists of laminated tantalum plates packed in a stainless steel case 3.6 cm x 4.8 cm x 7.5 cm length through which cooling water flows. The neutron moderator is mainly water in a reentrant aluminum case 20 cm diameter and about 5 cm width along the flight path direction, surrounded by boron-polyethylene plates. In order to diminish gamma flash onto the TOF detectors, two sets of lead shadow rings each 5 cm high and 15 cm thick are placed on horizontal plane around the target. A lead plate 5 mm thick is also inserted in the 47 m neutron path to shield against soft gamma rays scattered from the moderator.

(Neutron flight Station)

Figure 2 shows the detector system in the 47 m station. The neutron beam is transmitted through an evacuated aluminum flight tube of 30 cm diameter to the 47 m station. Aluminum plates 1 mm thick are used as windows of the flight tube, though some resonance structures appear in neutron spectrum. The neutron beam 9 cm in diameter at the window of the 47 m station is further collimated to a diameter of 7 cm at the sample position with several collimators having B_4C lining of 1 cm thickness. The distance from center of the neutron source to the sample is 47.08 m within an accuracy of $\pm$0.5 cm. A boronnitride plate is inserted to filter out slower neutrons which overlap the subsequent timing program.

(Flux Monitor)

The neutron flux on the sample is monitored with a ^6Li glass transmission type flux monitor,[13] as indicated in fig.2. A circular ^6Li glass scintillator (NE908, 120 mm dia.X 3 mm thick) is cut and polished to chord

length 5 cm, to fit flat windows of 2" diameter photomultipliers EMI-9750KB which view the scintillator from both sides. Aluminum windows 0.1 mm thick are used in the effective area 9 cm in diameter of the flux monitor. The flux monitor is placed 1.1 m before the sample for which capture probability is measured. Neutron pulses from both photomultipliers are mixed and amplified, pulse-height selected, inverted, and sent to the acquisition system through a double-shield coaxial cable. The neutron pulses, through time-gate circuits which open between 102.6 and 205.0 μsec after bursts, are stored in a preset scaler of the time-analyzer, and the counting rate is recorded with a pen-recorder. Neutron transmission of the flux monitor was measured to be

$$T = (0.92 \pm 0.02) \exp(-(0.93 \pm 0.02)/\sqrt{E}) \quad \cdots\cdots\cdots (1)$$

from which the neutron detection efficiency η was obtained as

$$\eta = 1 - \exp(-(0.93 \pm 0.02)/\sqrt{E}) \quad \cdots\cdots\cdots (2)$$

except for multiple scattering effects, where E is the neutron energy in eV.

(Moxon-Rae Detector)

Capture gamma rays from the samples are detected by a Moxon-Rae detector[14] whose construction is shown in fig.2. Compton electrons emitted by the capture gamma rays in electron converters produce scintillation light in two layers of thin plastic scintillator(NE102) 0.5 mm thick. A 3 cm thick transparent lucite disk was used as a light guide for the first layer, and also as an electron converter for the second layer, and on top of the first layer a Li_2CO_3-paraffin block was placed as neutron stopper and electron converter. The scintillator stack was coupled with a 5" diameter photomultiplier EMI-9530QR. Two Moxon-Rae detectors of the same type were placed in symmetrical geometry within the shielding inner surfaces lined with 1 cm thick B_4C. Pulses from the detectors were mixed, amplified pulse-height selected, inverted, and sent to the time analyzer through a double-shield coaxial cable.

The detection probability of a neutron capture event on the sample, $\varepsilon\Omega$ (detector efficiency ε multiplied by solid angle Ω subtended at the sample), was calibrated in two ways. The first was by counting the gamma rays from the standard sources of ^{60}Co, ^{22}Na, ^{137}Cs, ^{65}Zn, ^{54}Mn, and ^{85}Sr, and, the second way by counting neutron capture gamma rays from the black resonances of Ag, Sb, Ho, and W exposed to neutron fluxes of which intensities were measured with the transmission-type flux monitor. The propotionality

of detection efficiency to gamma-ray energy was confirmed, and the calibration measurements in the two ways agree within ± 5.3%. Pulse hieght discrimination level was adjusted so that $\varepsilon\Omega$ was 1.40×10^{-2} for neutron capture on Tb-159 nuclei with energy release of 6.381 MeV.

(Transmission Detector)

Neutron transmission of the samples was measured with a $1\frac{1}{2}$" dia. x $\frac{1}{2}$"t ^{6}Li-galss scintillator (NE908) coupled with an RCA-8850 photomultiplier and a $4\frac{3}{8}$" dia. x $\frac{1}{4}$" t ^{6}Li-glass (NE908) scintillator coupled with an EMI-9579A 5" photomultiplier. They were placed 0.3 m behind the sample.
Signals from these detectors were stored simultaneously in two or four divided parts of the TMC-4096 analyzer.
The electronics and data flow diagram are shown in fig.3.

(Samples)

Terbium is a monoisotopic rare earth element (Z=65, A=159, 100%).
Two samples were used; a thin sample was 99.9% purity Tb_4O_7 powder of 0.29g/cm^2, packed to 1 mm thickness in an aluminum case, and a thick one was a metallic plate about 2 mm thick, as shown in table 1.
The sample was placed at the center of the detector shielding, inclined 45 degrees to the incident neutron beam.

(Measurements)

Measurements were made under conditions in table 2. The linac was operated at energy 100 MeV with peak current 0.3~1.8 A, beam pulse width 0.08~0.3μ sec and repetition rate 150 pps. The neutron production rate was 2×10^{10} neutrons per 0.1μsec burst; 2×10^{17} n/sec during pulse. Neutron flux at the 47 m station was about $0.1 / E^{0.74}$ neutrons/cm^2 eV per burst.

(Data Processing)

Accumulated data in the TMC-4096 analyzer were output to 7-tracks magnetic tape, which were then transfered to the core of a TOSBAC USC-3 computor,[15] with which the data were rewritten to 9-tracks magnetic tape.[16] Through the FACOM-U-200 computor, the data on the magnetic tape were sent to a large FACOM-230/75 computor at the computor center of JAERI, and stored in disk-file. Further data processing, resonance analyses, and some kind of plottings were made with FACOM-230/75 in remote batch operation,

using U-200 as a terminal station installed at the LINAC laboratory.

(Transmission Data)

Transmission T is obtained by dividing the sample-in-data(I) by open-beam-data(O) after normalization with flux monitor counts, with proper subtraction of the backgrounds, B_i and B_o.

$$T = (I - B_i)/(O - B_o) \quad \cdots\cdots\cdots (3)$$

The backgrounds were obtained from black resonances, such as 11.0, 24.6, 46.0 eV of Tb, 330 eV, 2.3 keV of Mn, 2.85 keV of Na, and were approximated by function A - B.t in the energy region concerned, where A and B are constants and t the flight time. For simplicity B_i and B_o were assumed to be equal. The time-of-flight versus energy relation was calibrated by a 5.903 keV resonance of aluminum, adjusting the signal delay time to the analyzer. Absolute accuracies of the flight path length and analyzer channel width were 1×10^{-4} and 9×10^{-5} respectively. After smoothing the open-beam data, the transmission for each channel was calculated and stored in a magnetic disk-file of FACOM-230/75.

Resonance analyses were made on the transmission data in disk-file with a program[17] modefied from the Atta-Harvey area analysis code[18] based on the single level Breit-Wigner formula.*)

From the transmission data of thin and thick terbium samples, $2g\Gamma_n^o$ were obtained for 207 levels below 1192 eV, and also Γ for large resonances.

Figure 4 shows example transmission raw data measured for the thick sample with analyzer channel width 0.125μsec in the energy region of 45 to about 2500 eV.

---

* The transmission dip area for a well separated resonance is equal to

$$A_t = \frac{\pi}{2} N \sigma_o \Gamma \qquad \text{for the thin sample}$$

$$A_t = \sqrt{\pi N \sigma_o \Gamma^2} \qquad \text{for the thick sample} \qquad (\sigma_o = 4\pi \lambda\!\!\!^{-2}\, g\, \Gamma_n / \Gamma)$$

from which

$$g\Gamma_n = (A_t)_{thin} / 2\pi^2 N \lambda\!\!\!^{-2}$$

$$g\Gamma_n\Gamma = (A_t)^2_{thick} / 4\pi^2 N \lambda\!\!\!^{-2} \qquad \text{where } 4\pi \lambda\!\!\!^{-2} = 2.60 \times 10^6/E(eV)$$

From measurements of thin and thick samples, $g\Gamma_n$, Γ_γ in case of $\Gamma_n \ll \Gamma_\gamma$; and Γ_n, Γ, and g in case of $\Gamma_n \gg \Gamma_\gamma$ are obtained.

(capture Data)

Capture yields for the thin terbium sample in the energy region of 45 to 220 eV are shown in fig.5, and for the thick sample in the region of 180 eV to 20 keV in fig.6; the resonance energies are for large resonances. For analysis of capture data, capture probability P_C for the sample was defined as

$$P_C = \frac{C}{(\varepsilon\Omega)\ T\ B} \cdot \frac{\eta}{M} \qquad \cdots\cdots\cdots \quad (4)$$

where C : net capture counts in the Moxon-Rae detector,
T : Transmission of the flux monitor,
B : attenuation of the neutron beam by air 1.1 m thick,
η : neutron detection efficiency of the flux monitor,
M : counts in the flux monitor at respective energies,
$\varepsilon\Omega$: detection probability of a capture event for the Moxon-Rae detector.

The neutron flux irradiating the samples was approximated by a function

$$F\ E^a \exp\ (-K/\sqrt{E}) \qquad \cdots\cdots\cdots \quad (5)$$

where F, a, and K are constants and E the neutron energy in eV. The values a = 0.74 and K = 2.93 were used in the energy region below 1.5 keV, with which the neutron flux were fitted within 3%. The energy spectrum of neutrons from the target was thus proportional to $E^{(a-1.5)}dE = E^{-0.76}dE$, which was harder than a sufficiently moderated spectrum of $E^{-1}dE$. The exponential term in eq.(5) is the attenuation factor due to 1/V absorbers in the beam, i.e. boron-nitride filter and ^{6}Li glass of the flux monitor.

For determination of the background in capture data, four sets of measurements were made. With and without manganese 'resonance filter' in the beam for terbium sample and for the equivalent lead sample in place of the terbium sample. These measurements enabled interpolation of the background between the notches of the resonance filter. Effects of the manganese-resonance beam filtration are shown in fig.7, where the neutron flux disappears in vicinities of 2.3, 1.08 and 0.33 keV resonances of Mn. Capture yields for lead sample are also shown in the figure, which are not sensitive to the irradiating neutron flux. And the values well coinside with the yeilds of the terbium sample at the notches of black resonance of manganese. The background in the yield of terbium samples is thus essentially the yield for the lead sample. After subtraction of the background, the net neutron capture probabilities for terbium samples were obtained for each

timing channel as described in eq.(4). From the capture probabilities obtained, resonance parameters were obtained from the capture area for each resonance.**)

A program CAFIT[19] was developed and used for the resonance parameter analyses in which the level width was searched by iteration for the calculated capture area to be equal to the observed one. The program is based on Monte-Carlo calculation considering the multiple scattering effects, and capture and scattering probabilities for neutrons incident on a disk sample inclined at arbitrary angle to the beam were calculated. Neutron width $\Gamma_n(J)$ corresponding to spin J(=1 or 2 for s-wave resonance) are calculated from the $g\Gamma_n$ value which is obtained by area analysis of the transmission data. With the program CAFIT total width Γ is obtained for both spins for input parameters E_o, $\Gamma_n(J)$, $g(J)$ and A_c, where E_o is resonance energy, $\Gamma_n(J)$ neutron width for spin J, $g(J)$ spin statistical factor for spin J, and A_c the capture area. In change of $\Gamma_n(J)$ to $\Gamma'_n(J)$, the total width $\Gamma'(J)$ is obtainable. As illustrated in fig.8, the favourable spins in (Γ, $g\Gamma_n$) plane are obtained as the most probable intersection of curves thus obtained and those by transmission area analyses on different sample thicknesses.

3. Results and Discussion

(Resonance Parameters)

Resonance parameters obtained below 1.2 keV are listed in table 3.

**) For a separate resonance, with thin sample, capture area can be written as $A_c = \pi N \sigma_o \Gamma_\gamma / 2$ from which ($\sigma_o = 4\pi \lambda\!\!\!^{-2} g\Gamma_n / \Gamma$)

$$g\Gamma_n \Gamma_\gamma / \Gamma = A_c / 2\pi^2 N \lambda\!\!\!^{-2}$$

Similarly, scattering area is

$$A_s = \pi N \sigma_o \Gamma_n / 2$$

$$g\Gamma_n^2 / \Gamma = A_s / 2\pi^2 N \lambda\!\!\!^{-2}$$

In case of thick sample, however, multiple scattering effects disturb the above relation drastically.*

timing channel as described in eq.(4). From the capture probabilities obtained, resonance parameters were obtained from the capture area for each resonance.**)

A program CAFIT[19] was developed and used for the resonance parameter analyses in which the level width was searched by iteration for the calculated capture area to be equal to the observed one. The program is based on Monte-Carlo calculation considering the multiple scattering effects, and capture and scattering probabilities for neutrons incident on a disk sample inclined at arbitrary angle to the beam were calculated. Neutron width $\Gamma_n(J)$ corresponding to spin J(=1 or 2 for s-wave resonance) are calculated from the $g\Gamma_n$ value which is obtained by area analysis of the transmission data. With the program CAFIT total width Γ is obtained for both spins for input parameters E_o, $\Gamma_n(J)$, $g(J)$ and A_c, where E_o is resonance energy, $\Gamma_n(J)$ neutron width for spin J, $g(J)$ spin statistical factor for spin J, and A_c the capture area. In change of $\Gamma_n(J)$ to $\Gamma'_n(J)$, the total width $\Gamma'(J)$ is obtainable. As illustrated in fig.8, the favourable spins in (Γ, $g\Gamma_n$) plane are obtained as the most probable intersection of curves thus obtained and those by transmission area analyses on different sample thicknesses.

3. Results and Discussion

(Resonance Parameters)

Resonance parameters obtained below 1.2 keV are listed in table 3.

**) For a separate resonance, with thin sample, capture area can be written as $A_c = \pi N \sigma_o \Gamma_\gamma / 2$ from which ($\sigma_o = 4\pi \lambda\!\!\!^{-2} g\Gamma_n / \Gamma$)

$$g\Gamma_n \Gamma_\gamma / \Gamma = A_c / 2\pi^2 N \lambda\!\!\!^{-2}$$

Similarly, scattering area is

$$A_s = \pi N \sigma_o \Gamma_n / 2$$

$$g\Gamma_n^2 / \Gamma = A_s / 2\pi^2 N \lambda\!\!\!^{-2}$$

In case of thick sample, however, multiple scattering effects disturb the above relation drastically.*

Beyond Derrien's measurement, 50 new levels are analyzed between 754 and 1192 eV. In the overlapping region, the agreement in resonance energies is very good and that in $2g\Gamma_n^o$ is fairly good with those by Derrien of 21 753 eV, and those by Popov of 21 580 eV, except at very small resonances. Broad levels at 137.6, 404.5, 593, 1172 eV seemed to be doublets, but the level parameters were obtained as singlets. Two small levels at 4.27 and 39.10 eV as shown in fig.9 are inconsistent in strengths reported by some laboratories, so that it may due to tantalum impurity of about 0.25% atomic density.

(Level Density)

Figure 10 shows the cumulative number of resonances vs. neutron energy. To check the level detection for neutron energy, several thresheold values in $2g\Gamma_n^o$ are examined. For i-th level, if $2g\Gamma_n^o$ is greater than V_t, the level is counted as one level, and if not the level is rejected from cumulation. Fairly uniform distribution of levels over the neutron energy region is indicated in fig.10, though small levels are missed depending on detectability of the measureing system. The threshold values V_t are taken to be 0, 0.5, 1.0 and 1.5 $(meV)^{1/2}$ in this case. The average level spacing $D(V_t)$ are $D(0) = 4.3$ eV below 600 eV, and $D(1.0)$ and $D(1.5)$ are equal to 11.9 and 14.6 eV respectively in the region below 1.2 keV. If the reduced with $2g\Gamma_n^o$ is assumed to obey the Porter-Thomas distribution[20]

$$\rho(x)dx = \frac{1}{\sqrt{2\pi}} x^{-1/2} \exp(-x/2)\, dx \qquad \cdots\cdots\cdots \quad (6)$$

where $x = 2g\Gamma_n^o / \langle 2g\Gamma_n^o \rangle$ and $\int_0^\infty \rho(x)dx = 1$,

density of levels $1/D(V_t)$ is given by

$$1/D(V_t) = 1/D(0) \cdot \int_p^\infty \rho(x)dx = 2(1/D(0))\left\{ 1 - \frac{1}{\sqrt{2\pi}} \int_{-\infty}^{\sqrt{p}} \exp(-y^2/2)dy \right\} \quad \cdots\cdots (7)$$

where $p = V_t / \langle 2g\,\Gamma_n^o \rangle$.

From the observed level spacing $D(V_t)$, $\langle 2g\Gamma_n^o \rangle$ is estimated to be $\langle 2g\Gamma_n^o \rangle = 1.2 \pm 0.05$, which is consistent with the value $2\,S_o\,D(0) = 1.33 \pm 0.2$ $(meV)^{1/2}$.

(Strength Function)

The cumulative value of $2g\Gamma_n^o$ vs. neutron energy up to 1192 eV is shown in fig.11. As Tb-159 exists near a 4s peak of the strength function, all the levels except very small ones are thought to be s-wave resonances. In the energy region below 1.2 keV, the s-wave strength function S_o averaged over spin 1 and 2 is obtained to be

$$S_o = \left\langle \frac{\Gamma_n^o}{D} \right\rangle = \frac{\Sigma g\ \Gamma_n^o}{E_2 - E_1} = (\ 1.55 \pm 0.15\ )10^{-4} \quad \cdots\cdots\cdots \quad (8)$$

Which is in good agreement with Derrien's $(1.56 \pm 0.2)10^{-4}$ obtained below 753 eV, but not with Popov's $(1.25 \pm 0.18)10^{-4}$ obtained below 580 eV. The S_o obtained is in good agreement with that expected from the optical model[21].

($2g\Gamma_n^o$ Distribution)

The distribution of $2g\Gamma_n^o$ is shown in fig.12a with Porter-Thomas distribution curve[20]. In the figure a resonance at 1172 eV is omitted because of its anomalously large $2g\Gamma_n^o$ which is probably a doublet not separated in the present measurement.

(Level Spacing Distribution)

The nearest neighbour level spacing distribution for levels below 1.2 keV is shown in fig.12b, though an appreciable number of levels may be missed in the region above 600 eV. The Wigner and the random distributions are shown for comparison. In the case of mixed spin, the distribution function is expected to be a linear combination of these two. A histogram of the distribution for actual Tb-159 resonance levels shows peaks in the region of 2.0 to 3.0 eV and of 5.0 to 5.5 eV. Similar peaks appear for many nuclei[22], and some of them deviate from statistical distributions of resonance levels[23]. Figure 12c shows the level spacing distribution for two arbitrary levels; $D_{ij} = E_j - E_i$ (i=1,2,3,....., N-1: j=i+1, i+2, ..., N). In this case, no appreciable deviation from the average value is seen.

(Average Capture Cross Section)

Average capture cross section of Tb-159 was obtained from net neutron capture events and incident neutron flux. Net captures were obtained by suitable subtraction of the background estimated from the yield for the lead sample of equivalent thickness. Self-shielding effect was corrected for with the assumption $\Gamma_\gamma/\Gamma \simeq 1$.

$$\sigma_c(E) = -\frac{1}{N} \ln(1 - N\sigma_m(E)) = -\frac{1}{N} \ln\left(1 - \frac{C(E)}{\varepsilon\Omega\Phi\ (E)}\right) \quad \cdots\cdots \quad (10)$$

where $\sigma_c(E)$ is the corrected capture cross section, N the sample thickness in atoms/barn, $\sigma_m(E)$ the apparent capture cross section, C(E) the capture yield in the Moxon-Rae detector, $\Phi(E)$ the neutron fluence on the sample, and $\varepsilon\Omega$ the detection probability of a capture event. $\langle\sigma_c(E)\rangle$ were obtained by averaging TOF channel in several tens of channels. In fig.13 the average capture cross sections thus obtained are shown. A bump at 1.5 keV is seen

in $\sigma_c(E)$, which corresponds to a cluster of strong levels as shown in fig.6. The bump is also seen in the data of Block et al.[9] though the absolute values are different from the present authors'.

(Comparison of Data)

To compare JAERI data with those of SACLAY quantatively, in fig.14a $2g\Gamma_n^o$ for large resonances are plotted, with SACLAY's as ordinate and JAERI's as abscissa. As expected, each point is in the vicinity of a line inclined at an angle about 45 degrees as shown in fig.14a. Similar plot in Γ_γ is shown in fig.14b.

(Γ_γ Distribution)

Using the CAFIT program total width Γ were obtained from capture peak areas for large resonances. Average radiation width $\langle\Gamma_\gamma\rangle$ is obtained to be $\langle\Gamma_\gamma\rangle = 107 \pm 7$ meV for lower 25 levels of which spins are known. This value is in good agreement with Derrien's value $\langle\Gamma_\gamma\rangle = 97.0 \pm 7.5$ meV within experimental error. Spin dependence of Γ_γ was shown to be $\langle\Gamma_\gamma\rangle_{j=1}=102 \pm 13$ meV and $\langle\Gamma_\gamma\rangle_{j=2}=109 \pm 8$ meV; no conclusive results are drawn, however, because of the poor statistical accuracy.

Jain et al.[10] found a correlation between Γ_n^o and yield ratio R, which was taken with low and high pulse height bias for capture gamma ray spectra measured by NaI(Tl) detectors. They also found that intermediate structures in R, peak at about 180 eV neutron energy with width about 40 eV. In the present measurements on total Γ_γ, no significant structure was detected in about 180 eV region. Mizumoto et al.[11] observed capture gamma ray multiplicity $\bar{m}$ for Tb-159 from 3 to 300 keV neutron energy at ORELA and found small value of $\bar{m} = 2.45 \pm 0.01$ at 4 keV neutron energy, most of the capturing states thus decay in two step cascades.
To clarify the above phenomena, further detailed, investigation is necessary in the future.

The authors would like to thank Dr. A.Asami for his interest in this work and careful reading of the manuscript. They also thank the operation staffs for their skillful operation of the linac.

References

1. J.A.Harvey, D.J.Hughes, R.S.Carter, and V.E.Pilcher; phys.Rev. 99(1955)10
2. Wang-Nai-Yen, N.Iliescu, E.N.Karzhavina, Kim Hi San, A.B.Popov, L.B.Pikelner, T.Stadnikov, E.I.Sharapov, and Yu.S.Yazvitskii; Zhur.Eksp. i.Teoret.Fiz. 47(1964)43, (Transl. in Soviet-Phys. JETP 20(1965)30)
3. M.Asgher, M.C.Moxon and C.M.Chaffey; Conf on Study of Nuclear Structure with Neutrons, Antwerp, 1965 paper 65.
4. BNL-325 3rd ed.
5. H.Derrien and M.Alix; CEA-N-1867(1976)
6. A.B.Popov, H.Faikov, and H.Cher Gou ; JINR-P3-9743(1976), Yader.Phys. 26 (1977)14
7. B.P.Alfimenkov, G.G.Akopyan, V.A.Badov, A.I.Ibanenko, L.Lason, Y.D.Mareev, N.I.Moreba, O.I.Obchinikov, L.B.Pikenlner, Sya.Salai, and E.I.Sharapov; JINR-P3-9852(1976), Yader. Phys. 25(1977)930
8. J.H.Gibbon, R.L.Macklin, P.D.Miller, and J.H.Neiler; Phys. Rev. 122(1961)1
9. R.C.Block, G.G.Slaughter, L.W.Watson, and F.C.Vanderlage; ORNL-3085(1961)
10. A.P.Jain, B.Cauvin, and A.Lottin; Nucl. Phys. A223(1974)509
11. M.Mizumoto, R.L.Macklin and J.Halperin; Submitted to Phys. Rev.
12. H.Takekoshi ed; JAERI-Report 1238(1975)
13. M.Ohkubo; JAERI-M 6630(1976)
14. M.Ohkubo; JAERI-M 6918(1977)
15. Y.Kawarasaki, T.Shoji, and M.Mizumoto; JAERI-M 5572(1974)
16. Y.Kawarasaki; JAERI-M 5435(1973)
17. A.Tachibana, T.Iwaki, E.Kimura, A.Asami, Y.Nakajima and T.Fuketa; JAERI-memo 3728(1969)
18. S.Atta and J.A.Harvey; ORNL-3205(1961)
19. M.Ohkubo; to be published in JAERI-M
20. C.E.Porter and R.G.Thomas; Phys. Rev. 104(1956)483
21. B.Block, H.Feshbach; Ann. Phys. 23(1963)47
22. W.W.Havens; "Progress in fast neutron Physics" G.G.Phillips, J.B.Marion J.R.Risser ed. The Univ. Chicage Press 1963. p.215
23. K.Ideno and M.Ohkubo; J.Phys. Soc. Japan 30(1971)620, K.Ideno; ibid.37 (1974)581
24. J.B.Czirr and M.L.Stelts; Nucl. Sci. Eng. 52(1973)299

Figure Captions

Fig.1 Schematic figure of the JAERI linac TOF facility, and a sketch of the target assembly.

Fig.2 Arrangement in the 47 m station. Moxon-Rae detector is shown in bottom right.

Fig.3 Electronics block diagram.

Fig.4 Transmission raw data for the sample-B in the region from 45 to 2500 eV with channel width 0.125μsec.

Fig.5 Capture raw data for sample-A in the energy region from 45 to 220 eV with channel width 0.25μsec.

Fig.6 Capture raw data for sample-B up to 20 keV with channel width 0.125μsec.

Fig.7 Upper figure: Capture raw data for Tb sample-B exposed to Mn-filtered beam, where neutron flux vanishes in the vicinity of 2.3, 1.08, and 0.33 keV resonances of Mn. Capture yield for an equivalent lead sample is also shown, which is not sensitive to the neutron flux variation, and it approximately coincides with the yield of terbium sample at the notches of the black resonances of Mn. Lower figure: Effect of the Mn resonance filter on the neutron beam measured by the ^{6}Li-glass detector when the capture sample is not.

Fig.8 Examples of resonance parameter analyses. a) 45.99 eV, b) 108.99 eV, c) 113.6 eV, and d) 219.0 eV. The curves T_A, T_B are obtained from transmission area analyses for sample A and B. The curves C_A and C_B are obtained by capture area analyses for sample A and B with CAFIT for spin J=1, and 2. Curves CB, in fig.c 'single' means that the analyses are made as isolated single level, and 'multi' means that the analyses are made as a member of several neighbouring levels. In fact 'multi' is more realistic.

Fig.9 Transmission and capture raw data in the energy region above 3 eV.

Fig 10 Cumulative number of resonances vs. neutron energy up to 1.2 keV. Threshold values in $2g\Gamma_n^o$ are 0, 0.5, 1.0, and 1.5$(meV)^{1/2}$.

Fig.11 Cumulative value of $2g\Gamma_n^o$ vs. neutron energy up to 1.2 keV.

Fig.12a. Reduced neutron width $(2g\Gamma_n^o)$ distribution for the level below 1.2 keV. Average value and the Porter-Thomas distribution curve are shown.

Fig.12b. Spacing distribution between adjacent levels. Average value and the Wigner and Random distributions are also shown.

Fig.12c. Spacing distribution between arbitrary two levels.

Fig. 13 Average capture cross section up to 30 keV. The values by other authers are also shown.

Fig.14a Comparison of JAERI and SACLAY data for each resonances. Plot of $2g\Gamma_n^o$, with ordinate SACLAY values and in abscissa JAERI values.

Fig.14b Plot of Γ_γ for each resonance, with ordinate SACLAY values and in abscissa JAERI values.

Table 1. Samples used

Sample A	Terbium Oxcide(Tb_4O_7) powder packed in an aluminum case. 0.000928 atoms/barn normal to the sample surface, 0.00131 atoms/barn for inclination of 45 degrees to the neutron beam.
Sample B	Terbium metallic plate 0.00789 atoms/barn normal to the sample surface, 0.0112 atoms/barn for inclination of 45 degrees to the neutron beam.

Table 2. Condition of Measurements

Energy Region Analyzed	Linac Pulse Width	Analyzer Channel Width
1 ~ 100 eV	0.1μsec	1μsec
46 ~ 200	0.1	0.25
185 ~ 1200	0.08	0.125

Table3. List of Resonance Parameters

JAERI NEUTRON RESONANCE PARAMETERS, TB-159, M.OHKUBO + Y.KAWARASAKI 1976-77
LI-6 GLASS,MOXON-RAE DET,0.00131,0.0112A/B 1,0.25,0.125MUS/CHANL,47M STAT TOF

	ENERGY(EV)	DE	F*G*GN0	D(F*G*GN0)	GAM.T	D(GAM.T)	GAM.G	D(GAM.G)	G	LAB
1	3.339	0.005	0.25	0.01	95.	10.	94.	10.	/	JAE
2	4.26	0.01	0.0035	0.001					/	---
3	4.97	0.01	0.028	0.003					/	JAE
4	11.07	0.02	2.80	0.15	115.	15.	107.	15.	/	JAE
5	14.40	0.02	0.05	0.006					/	JAE
6	21.17	0.03	0.32	0.025	95.	10.	94.	10.	/	JAE
7	24.56	0.04	1.05	0.07	110.	10.	106.	10.	/	JAE
8	27.51	0.04	0.19	0.016					/	JAE
9	33.81	0.05	0.46	0.03	120.	15.	116.	15.	/	JAE
10	39.10	0.05	0.022	0.002					/	---
11	40.72	0.05	0.095	0.005					/	JAE
12	43.63	0.06	0.77	0.05	118.	10.	114.	10.	/	JAE
13	45.99	0.03	2.00	0.10	113.	10.	102.	10.	/	JAE
14	50.06	0.03	0.31	0.03					/	JAE
15	51.56	0.03	0.15	0.010					/	JAE
16	53.98	0.03	0.085	0.01					/	JAE
17	57.34	0.03	0.20	0.016					/	JAE
18	58.63	0.03	0.25	0.02					/	JAE
19	65.08	0.03	1.28	0.1	115.	15.	107.	15.	/	JAE
20	66.48	0.04	0.32	0.03					/	JAE
21	73.66	0.04	2.0	0.12	133.	15.	120.	15.	5/8	JAE
22	76.31	0.04	0.70	0.06					/	JAE
23	77.75	0.05	0.75	0.05	115.	15.	110.	15.	/	JAE
24	78.60	0.05	0.21	0.02					/	JAE
25	88.26	0.06	0.41	0.04	120.	15.	117.	15.	/	JAE
26	90.31	0.06	0.90	0.09	117.	15.	106.	15.	/	JAE
27	95.31	0.07	0.07	0.01					/	JAE
28	96.95	0.07	3.1	0.2	133.	10.	92.	10.	3/8	JAE
29	108.99	0.07	2.8	0.3	125.	10.	102.	10.	5/8	JAE
30	111.17	0.09	0.58	0.04					/	JAE
31	113.61	0.09	3.90	0.3	145.	10.	90.	10.	3/8	JAE
32	115.40	0.09	0.70	0.06					/	JAE
33	119.06	0.09	1.18	0.07	130.	15.	120.	15.	5/8	JAE
34	128.13	0.10	0.085	0.01					/	JAE
35	137.75	0.10	0.90	0.15					/	JAE
36	141.16	0.1	2.3	0.2	130.	15.	108.	15.	5/8	JAE
37	143.33	0.12	1.00	0.1	110.	15.	94.	15.	3/8	JAE
38	152.52	0.13	2.0	0.2	130.	15.	97.	15.	3/8	JAE
39	155.43	0.14	2.2	0.2	125.	15.	103.	15.	5/8	JAE
40	167.47	0.15	0.12	0.01					/	JAE

JAERI NEUTRON RESONANCE PARAMETERS, TB-159, M.OHKUBO + Y.KAWARASAKI 1976-77
LI-6 GLASS,MOXON-RAE DET,0.00131,0.0112A/B 1,0.25,0.125MUS/CHANL.47M STAT TOF

	ENERGY(EV)	DE	F*G*GNO	D(F*G*GNO)	GAM.T	D(GAM.T)	GAM.G	D(GAM.G)	G	LAB
41	169.63	0.15	0.52	0.05					/	JAE
42	172.57	0.17	0.19	0.02					/	JAE
43	177.30	0.17	1.44	0.09	120.	15.	105.	15.	/	JAE
44	185.41	0.1	0.13	0.01					/	JAE
45	197.36	0.10	1.20	0.08	115.	15.	102.	15.	/	JAE
46	199.6	0.1	0.27	0.02					/	JAE
47	201.40	0.1	0.20	0.02					/	JAE
48	210.8	0.1	0.10	0.01					/	JAE
49	216.89	0.1	0.2	0.05					/	JAE
50	219.0	0.1	5.5	0.5	185.	15.	120.	15.	5/8	JAE
51	225.9	0.1	0.1	0.02					/	JAE
52	228.4	0.1	0.05	0.005					/	JAE
53	232.4	0.1	0.16	0.02					/	JAE
54	235.1	0.1	2.1	0.3	145.	15.	120.	15.	5/8	JAE
55	238.6	0.1	2.5	0.4	180.	15.	123.	15.	3/8	JAE
56	241.5	0.1	0.90	0.1					/	JAE
57	244.4	0.1	0.06	0.01					/	JAE
58	251.2	0.1	0.45	0.05					/	JAE
59	254.1	0.1	0.16	0.02					/	JAE
60	262.9	0.2	1.6	0.2					/	JAE
61	263.8	0.2	0.2	0.05					/	JAE
62	268.4	0.2	0.5	0.05					/	JAE
63	273.4	0.2	2.0	0.2					/	JAE
64	279.8	0.2	0.15	0.05					/	JAE
65	281.3	0.2	0.9	0.1					/	JAE
66	282.6	0.2	0.1	0.05					/	JAE
67	284.2	0.2	7.5	0.8					/	JAE
68	285.4	0.2	0.15	0.05					/	JAE
69	290.2	0.2	0.75	0.08					/	JAE
70	300.8	0.2	2.10	0.20					/	JAE
71	305.5	0.2	1.30	0.15					/	JAE
72	310.7	0.2	0.15	0.05					/	JAE
73	312.1	0.2	2.60	0.30					/	JAE
74	315.4	0.2	0.20	0.05					/	JAE
75	323.2	0.2	0.90	0.10					/	JAE
76	325.5	0.2	0.70	0.10					/	JAE
77	328.0	0.2	3.50	0.5					/	JAE
78	331.9	0.2	3.2	0.5					/	JAE
79	336.8	0.2	0.1	0.02					/	JAE
80	339.3	0.2	0.08	0.02					/	JAE

JAERI NEUTRON RESONANCE PARAMETERS, TB-159, M.OHKUBO + Y.KAWARASAKI 1976-77
LI-6 GLASS,MOXON-RAE DET,0.00131,0.0112A/B 1,0.25,0.125MUS/CHANL,47M STAT TOF

	ENERGY(EV)	DE	F*G*GNO	D(F*G*GNO)	GAM.T	D(GAM.T)	GAM.G	D(GAM.G)	G	LAB
81	345.3	0.2	0.6	0.1					/	JAE
82	347.5	0.2	2.8	0.3					/	JAE
83	349.9	0.2	0.45	0.05					/	JAE
84	356.8	0.2	0.85	0.1					/	JAE
85	358.8	0.2	4.2	0.4					/	JAE
86	361.4	0.2	0.08	0.01					/	JAE
87	366.4	0.3	0.8	0.1					/	JAE
88	368.8	0.3	0.40	0.05					/	JAE
89	371.9	0.3	2.5	0.25					/	JAE
90	374.2	0.3	1.5	0.2					/	JAE
91	378.2	0.2	6.0	0.8					/	JAE
92	381.2	0.3	0.15	0.02					/	JAE
93	384.8	0.3	0.3	0.03					/	JAE
94	404.5	0.3	3.7	0.5					/	JAE
95	409.1	0.3	0.7	0.07					/	JAE
96	415.9	0.3	3.0	0.3					/	JAE
97	421.1	0.3	0.12	0.03					/	JAE
98	432.5	0.3	0.6	0.06					/	JAE
99	434.5	0.4	0.10	0.03					/	JAE
100	440.1	0.4	1.35	0.13					/	JAE
101	442.6	0.4	1.2	0.2					/	JAE
102	444.7	0.4	0.4	0.1					/	JAE
103	451.0	0.4	0.2	0.1					/	JAE
104	453.1	0.4	3.2	0.3					/	JAE
105	457.7	0.4	0.8	0.08					/	JAE
106	462.2	0.4	0.1	0.05					/	JAE
107	463.6	0.4	0.1	0.05					/	JAE
108	468.0	0.4	4.7	0.5					/	JAE
109	474.1	0.4	1.3	0.1					/	JAE
110	476.8	0.4	0.2	0.1					/	JAE
111	480.4	0.4	2.0	0.5					/	JAE
112	482.0	0.4	5.0	1.0					/	JAE
113	488.7	0.4	5.0	1.0					/	JAE
114	494.0	0.4	1.2	0.1					/	JAE
115	498.0	0.4	0.60	0.05					/	JAE
116	503.1	0.4	1.4	0.15					/	JAE
117	510.1	0.4	1.2	0.10					/	JAE
118	517.5	0.4	0.4	0.1					/	JAE
119	520.9	0.4	2.2	0.2					/	JAE
120	527.9	0.4	2.0	0.2					/	JAE

JAERI NEUTRON RESONANCE PARAMETERS, TB-159, M.OHKUBO + Y.KAWARASAKI 1976-77
LI-6 GLASS,MOXON-RAE DET,0.00131,0.0112A/B 1,0.25,0.125MUS/CHANL,47M STAT TOF

	ENERGY(EV)	DE	F*G*GNO	D(F*G*GNO)	GAM.T	D(GAM.T)	GAM.G	D(GAM.G)	G	LAB
121	532.9	0.5	3.8	0.4					/	JAE
122	544.6	0.5	0.84	0.08					/	JAE
123	552.1	0.5	0.75	0.07					/	JAE
124	557.1	0.5	0.7	0.1					/	JAE
125	560.6	0.5	0.75	0.1					/	JAE
126	564.9	0.5	2.5	0.3					/	JAE
127	569.8	0.5	1.8	0.2					/	JAE
128	576.3	0.5	0.3	0.1					/	JAE
129	580.0	0.5	2.0	0.2					/	JAE
130	593.6	0.5	7.	1.					/	JAE
131	597.9	0.5	2.5	0.2					/	JAE
132	600.1	0.5	0.85	0.15					/	JAE
133	602.9	0.5	2.2	0.2					/	JAE
134	608.6	0.6	0.65	0.1					/	JAE
135	615.7	0.6	7.5	1.0					/	JAE
136	620.5	0.6	1.2	0.1					/	JAE
137	627.2	0.6	2.5	0.3					/	JAE
138	630.2	0.6	0.55	0.1					/	JAE
139	637.9	0.6	0.75	0.1					/	JAE
140	644.3	0.6	0.7	0.1					/	JAE
141	648.7	0.6	4.5	0.5					/	JAE
142	654.5	0.6	0.2	0.1					/	JAE
143	660.1	0.6	0.65	0.1					/	JAE
144	662.6	0.6	0.45	0.1					/	JAE
145	677.7	0.6	0.4	0.1					/	JAE
146	683.6	0.7	6.0	1.0					/	JAE
147	686.8	0.7	1.6	0.2					/	JAE
148	693.8	0.7	0.7	0.1					/	JAE
149	700.9	0.7	1.3	0.1					/	JAE
150	707.6	0.7	0.5	0.1					/	JAE
151	714.2	0.7	0.3	0.1					/	JAE
152	720.0	0.7	8.2	0.8					/	JAE
153	727.1	0.7	0.6	0.1					/	JAE
154	732.1	0.8	2.7	0.3					/	JAE
155	738.8	0.8	0.9	0.1					/	JAE
156	747.2	0.8	0.6	0.2					/	JAE
157	751.9	0.8	0.8	0.2					/	JAE
158	754.5	0.8	0.3	0.1					/	JAE
159	765.2	0.8	9.0	1.0					/	JAE
160	769.8	0.8	2.0	0.2					/	JAE

JAERI NEUTRON RESONANCE PARAMETERS, TB-159, M.OHKUBO + Y.KAWARASAKI 1976-77
LI-6 GLASS,MOXON-RAE DET,0.00131,0.0112A/B 1,0.25,0.125MUS/CHANL,47M STAT TOF

	ENERGY(EV)	DE	F*G*GNO	D(F*G*GNO)	GAM,T	D(GAM,T)	GAM,G	D(GAM,G)	G	LAR
161	782.5	0.8	0.3	0.1					/	JAE
162	787.7	0.8	3.8	0.4					/	JAE
163	793.0	0.9	0.5	0.1					/	JAE
164	802.0	0.9	2.7	0.3					/	JAE
165	810.2	0.9	2.1	0.2					/	JAE
166	815.7	0.9	0.4	0.1					/	JAE
167	823.9	0.9	2.5	0.3					/	JAE
168	837.0	0.9	0.3	0.1					/	JAE
169	845.3	0.9	6.0	0.6					/	JAE
170	850.5	0.9	3.3	0.3					/	JAE
171	855.9	0.9	0.5	0.2					/	JAE
172	861.4	1.0	0.8	0.2					/	JAE
173	869.8	1.0	0.3	0.1					/	JAE
174	875.4	1.0	0.4	0.1					/	JAE
175	884.7	1.0	2.2	0.2					/	JAE
176	896.4	1.0	0.8	0.2					/	JAE
177	901.5	1.0	2.7	0.3					/	JAE
178	912.5	1.0	0.35	0.1					/	JAE
179	924.9	1.0	4.5	0.5					/	JAE
180	936.0	1.1	9.0	1.0					/	JAE
181	944.4	1.1	0.3	0.1					/	JAE
182	951.3	1.1	1.6	0.2					/	JAE
183	955.3	1.1	0.5	0.2					/	JAE
184	963.2	1.1	7.0	1.0					/	JAE
185	968.4	1.1	1.0	0.5					/	JAE
186	972.6	1.1	2.2	0.2					/	JAE
187	980.2	1.1	3.7	0.4					/	JAE
188	995.2	1.2	10.	2.0					/	JAE
189	1000.7	1.2	2.0	0.3					/	JAE
190	1005.0	1.2	0.4	0.1					/	JAE
191	1016.2	1.2	1.0	0.1					/	JAE
192	1028.0	1.2	0.5	0.1					/	JAE
193	1036.3	1.2	1.5	0.5					/	JAE
194	1040.2	1.2	4.0	0.5					/	JAE
195	1050.0	1.3	4.5	0.5					/	JAE
196	1057.0	1.3	4.0	0.4					/	JAE
197	1067.7	1.3	1.5	0.5					/	JAE
198	1076.6	1.3	8.0	1.0					/	JAE
199	1097.6	1.3	2.5	0.3					/	JAE
200	1105.5	1.4	2.0	0.3					/	JAE

JAERI NEUTRON RESONANCE PARAMETERS, TB-159, M.OHKUBO + Y.KAWARASAKI 1976-77
LI-6 GLASS,MOXON-RAE DET,0.00131,0.0112A/B 1,0.25,0.125MUS/CHANL.47M STAT TOF

	ENERGY(EV)	DE	F*G*GNO	D(F*G*GNO)	GAM.T	D(GAM.T)	GAM.G	D(GAM.G)	G	LAB
201	1112.8	1.4	4.6	0.5					/	JAE
202	1124.1	1.4	1.8	0.3					/	JAE
203	1132.2	1.4	2.0	0.5					/	JAE
204	1142.7	1.4	0.5	0.2					/	JAE
205	1148.0	1.4	2.0	0.2					/	JAE
206	1157.0	1.5	1.0	0.2					/	JAE
207	1172.8	1.5	21.0	2.0					/	JAE
208	1184.4	1.5	2.0	0.2					/	JAE
209	1192.2	1.5	1.6	0.2					/	JAE

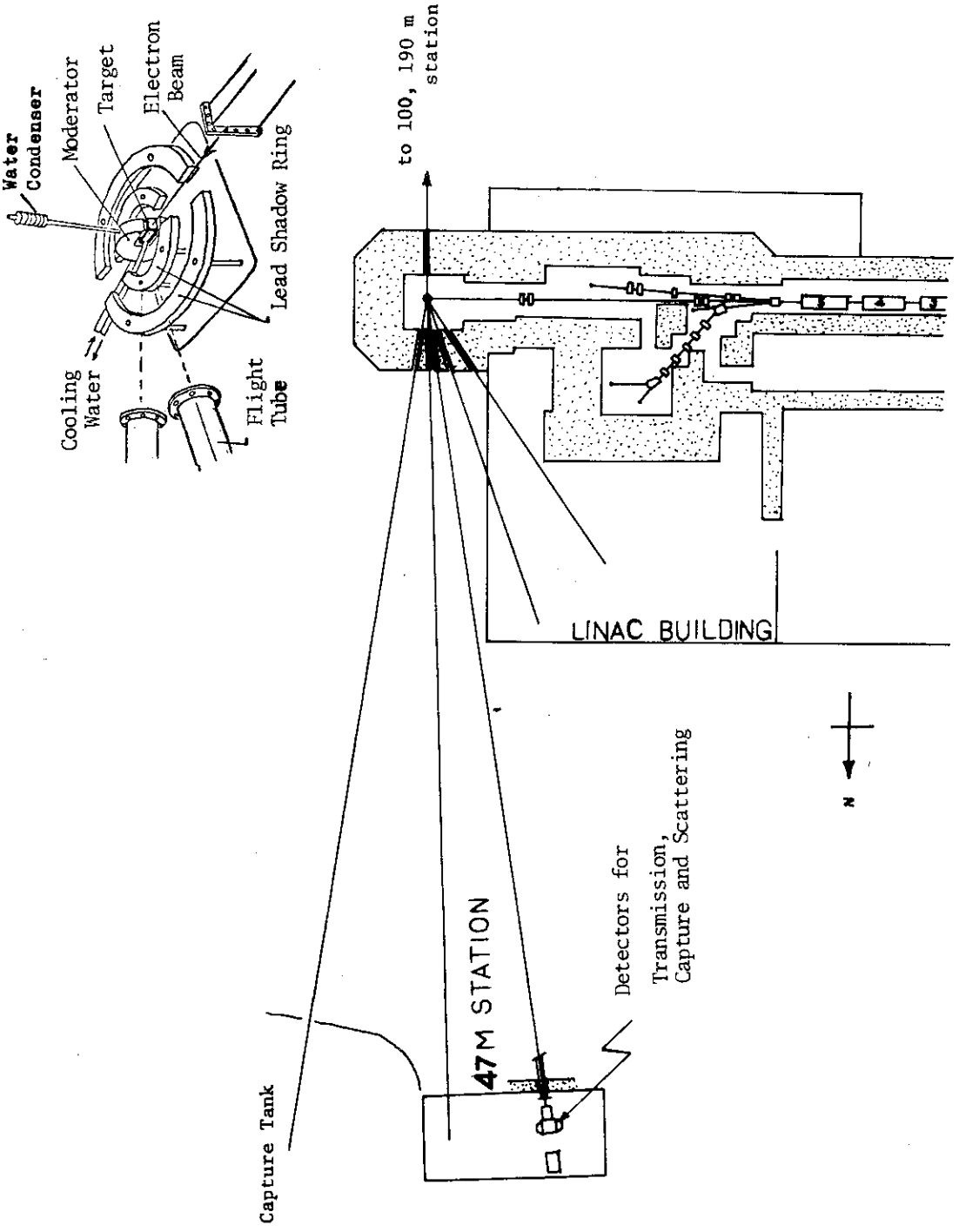

Fig.1 Schematic figure of the JAERI linac TOF facility, and a sketch of the target assembly.

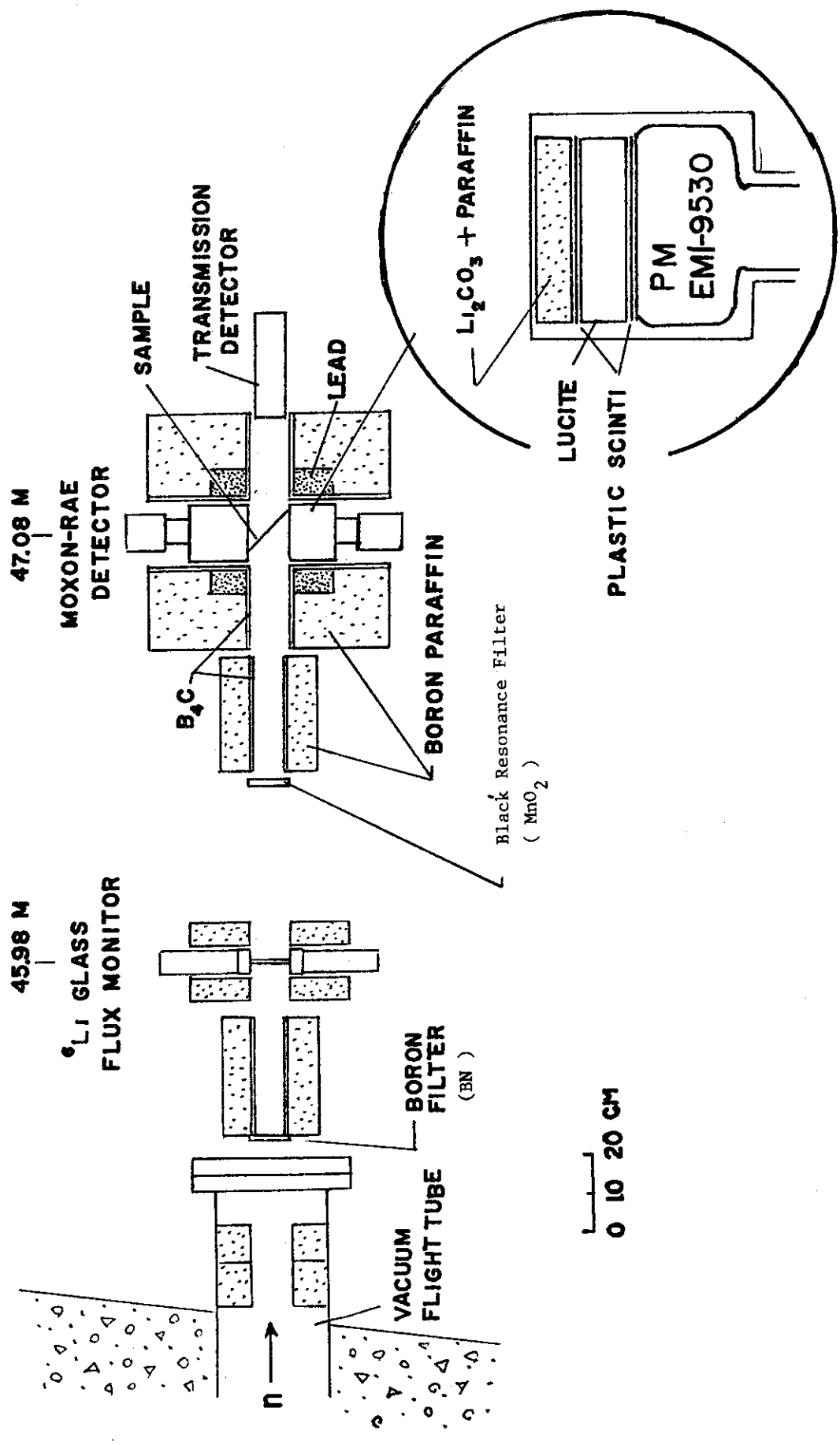

Fig.2 Arrangement in the 47 m station. Moxon-Rae detector is shown in bottom right.

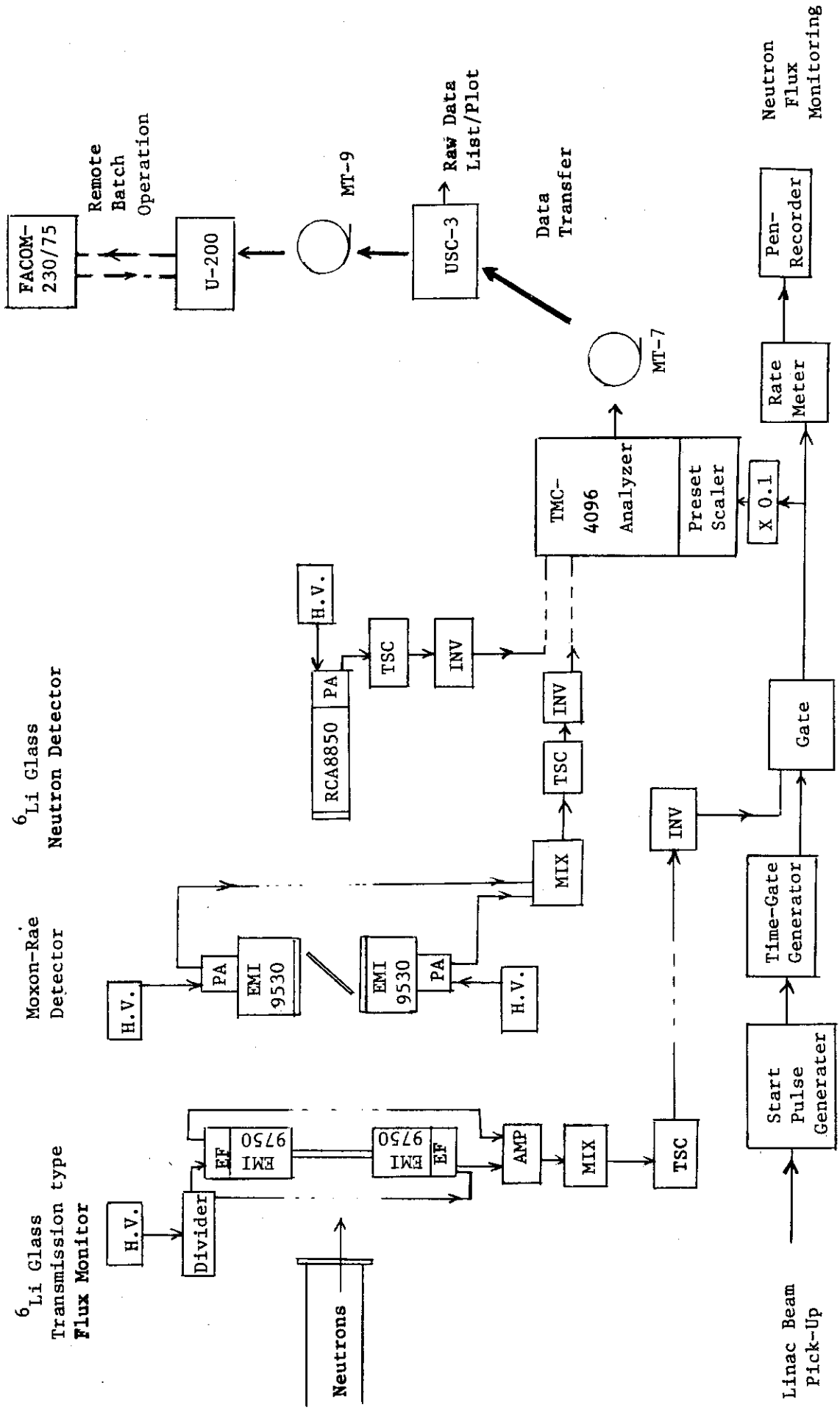

Fig.3 Electronics block diagram.

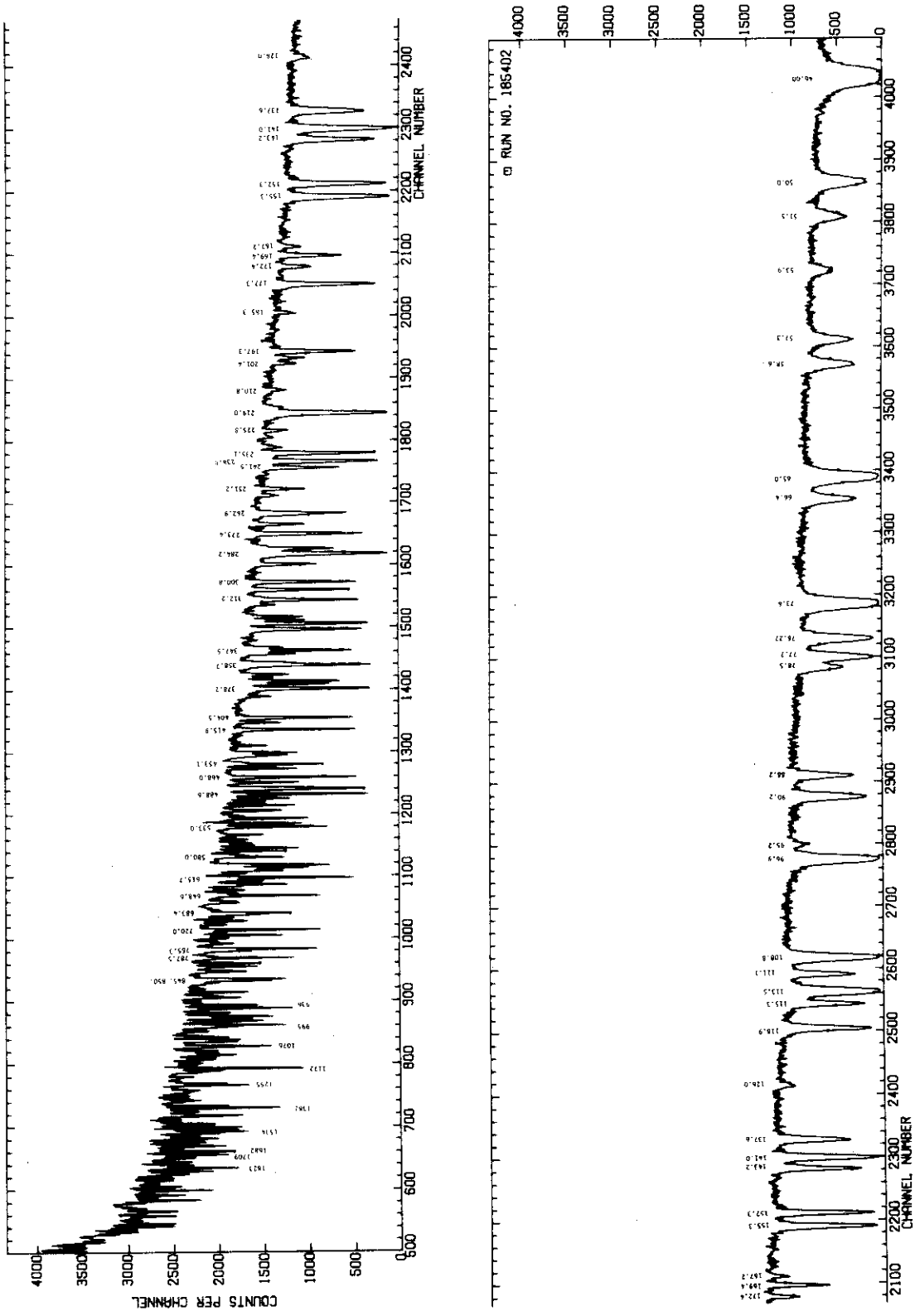

Fig.4 Transmission raw data for the sample-B in the region from 45 to 2500 eV with channel width 0.125μsec.

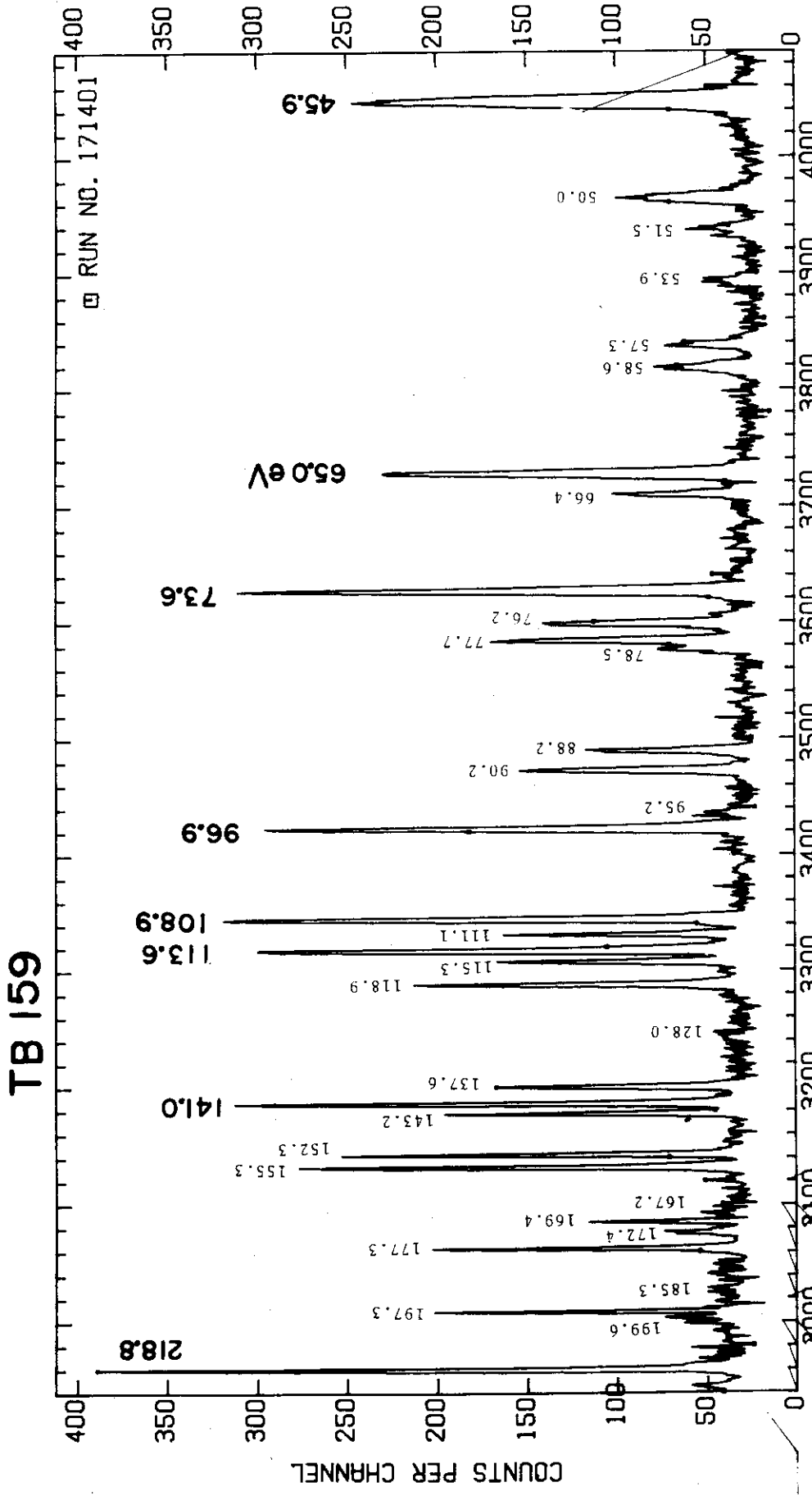

Fig.5 Capture raw data for sample-A in the energy region from 45 to 220 eV with channel width 0.25μsec.

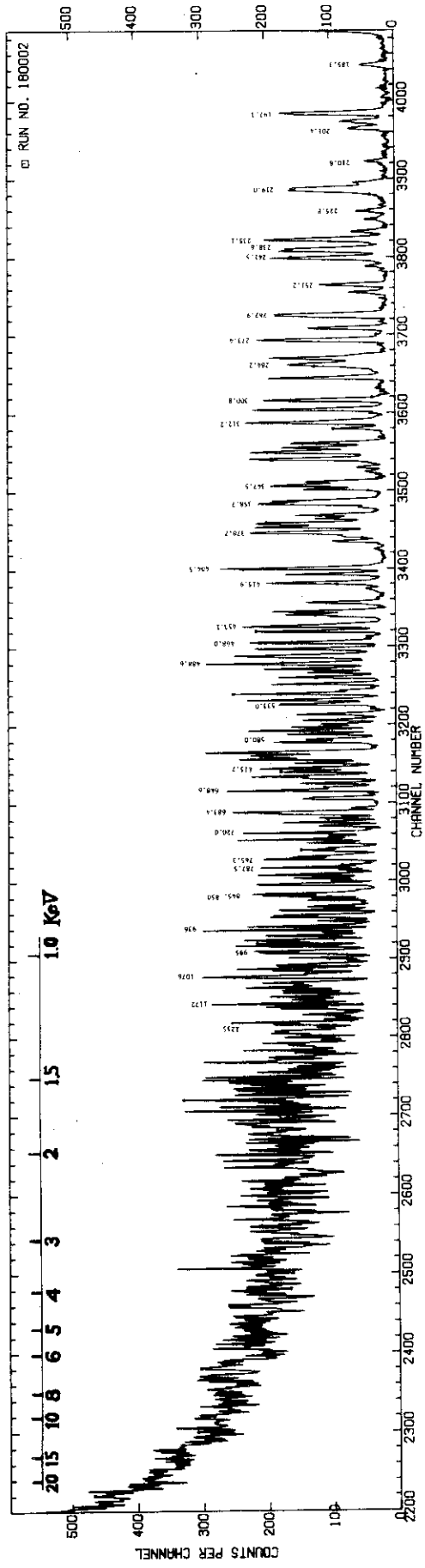

Fig.6 Capture raw data for sample-B up to 20 keV with channel width 0.125μsec.

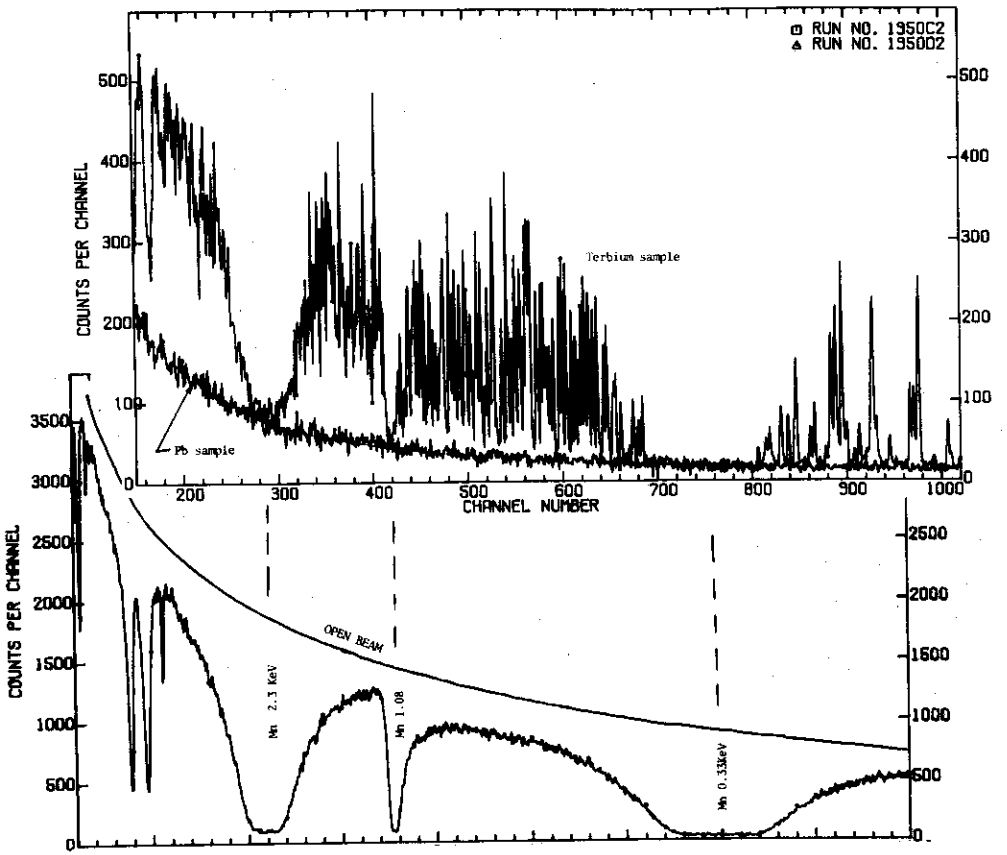

Fig.7 Upper figure: Capture raw data for Tb sample-B exposed to Mn-filtered beam, where neutron flux vanishes in the vicinity of 2.3, 1.08, and 0.33 keV resonances of Mn. Capture yield for an equivalent lead sample is also shown, which is not sensitive to the neutron flux variation, and it approximately coincides with the yield of terbium sample at the notches of the black resonances of Mn. Lower figure: Effect of the Mn resonance filter on the neutron beam measured by the ^{6}Li-glass detector when the capture sample is not.

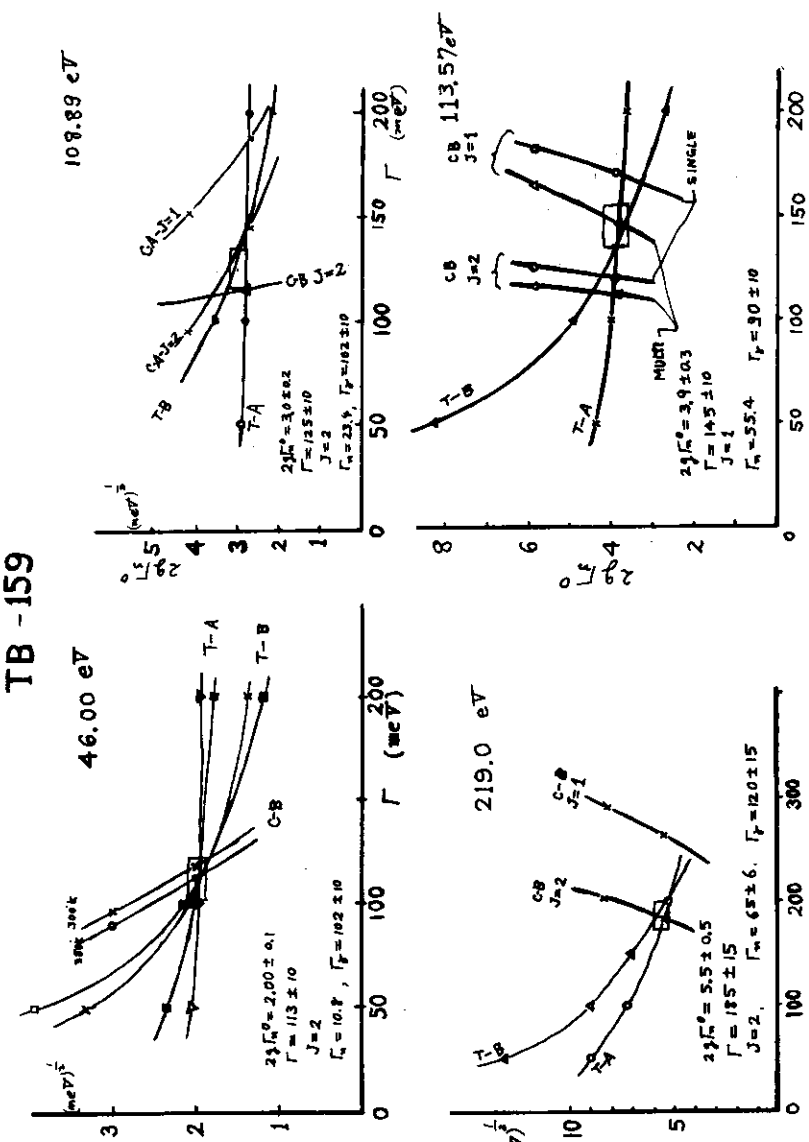

Fig.8 Examples of resonance parameter analyses. a) 45.99 eV, b) 108.99 eV, c) 113.6 eV, and d) 219.0 eV. The curves T_A, T_B are obtained from transmission area analyses for sample A and B. The curves C_A and C_B are obtained by capture area analyses for sample A and B with CAFIT for spin J=1, and 2. Curves CB, in fig.c 'single' means that the analyses are made as isolated single level, and 'multi' means that the analyses are made as a member of several neighbouring levels. In fact 'multi' is more realistic.

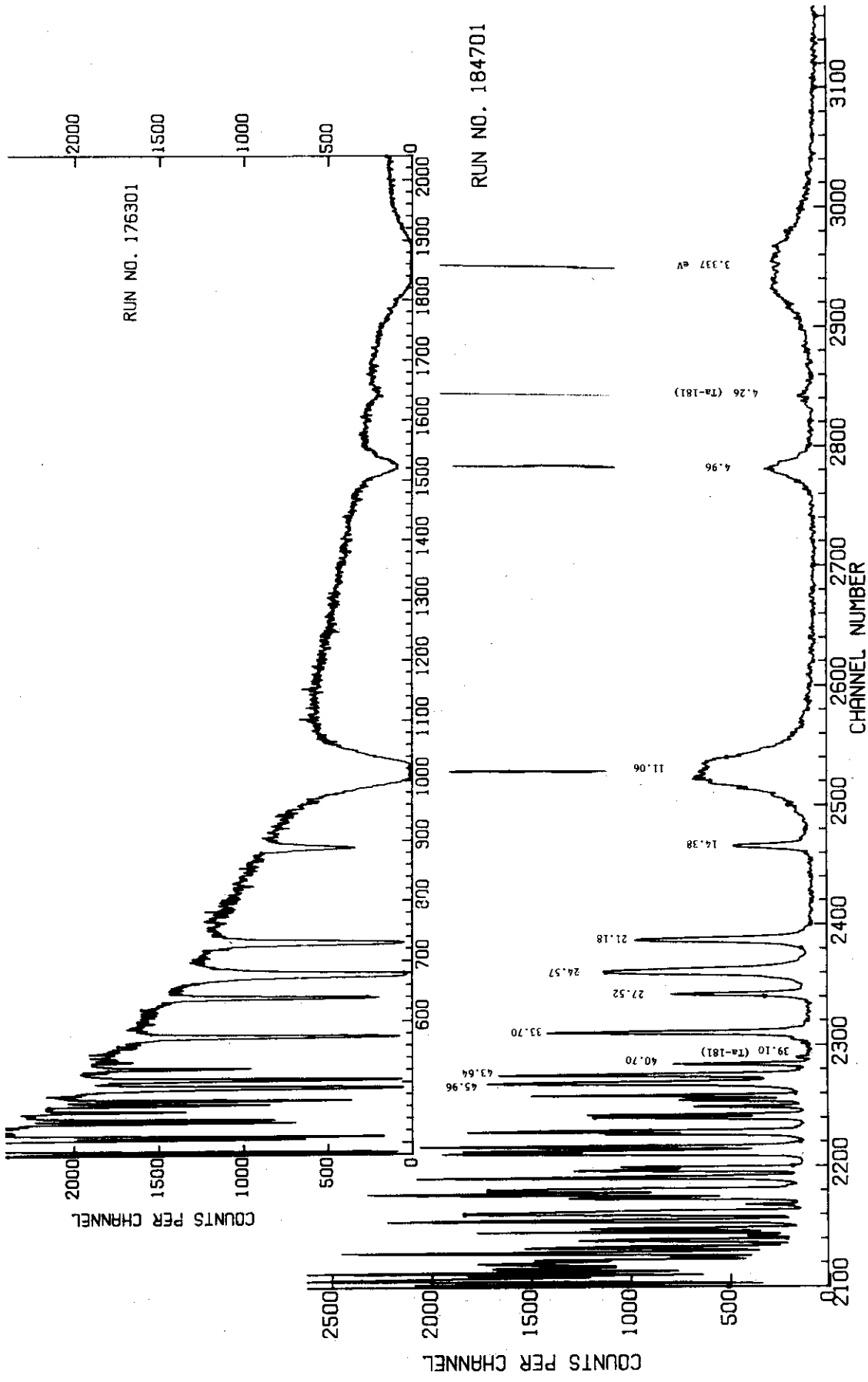

Fig.9 Transmission and capture raw data in the energy region above 3 eV.

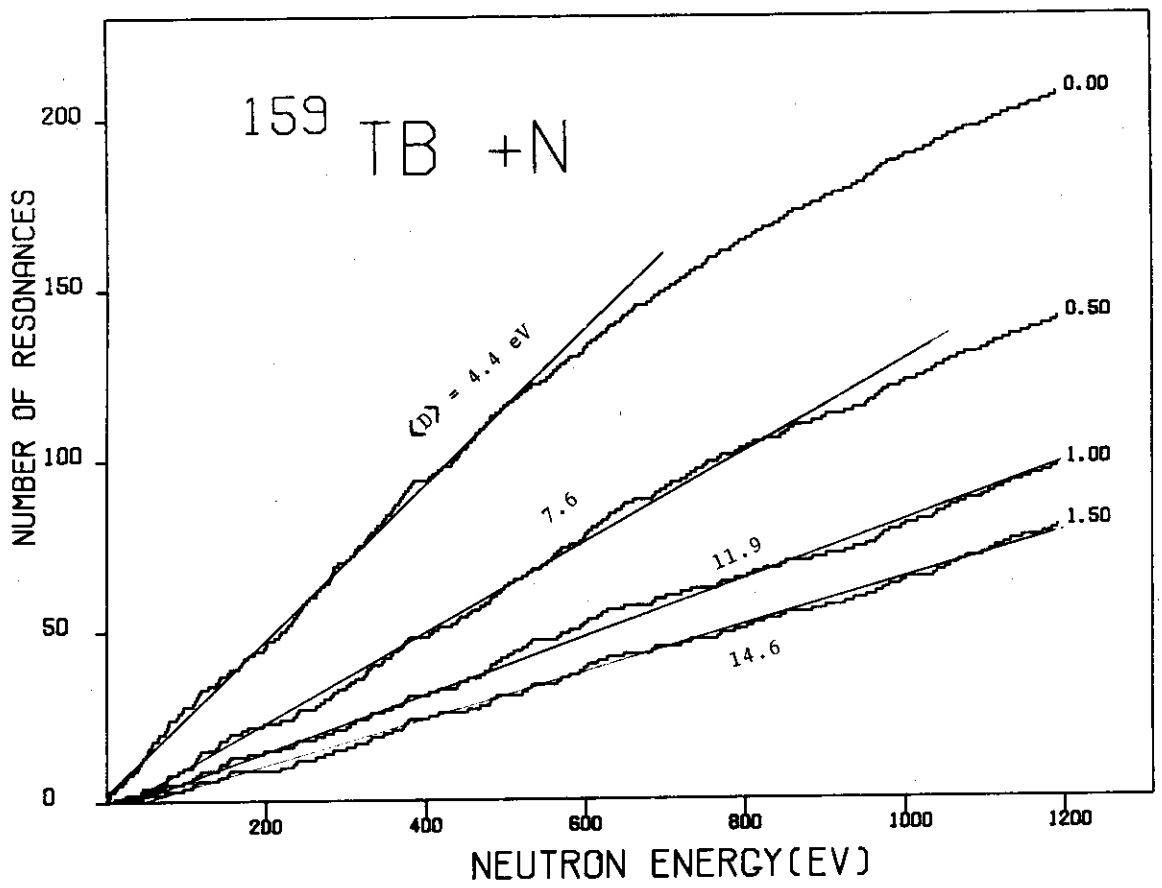

Fig 10 Cumulative number of resonances vs. neutron energy up to 1.2 keV. Threshold values in $2g\Gamma_n^o$ are 0, 0.5, 1.0, and 1.5$(meV)^{1/2}$.

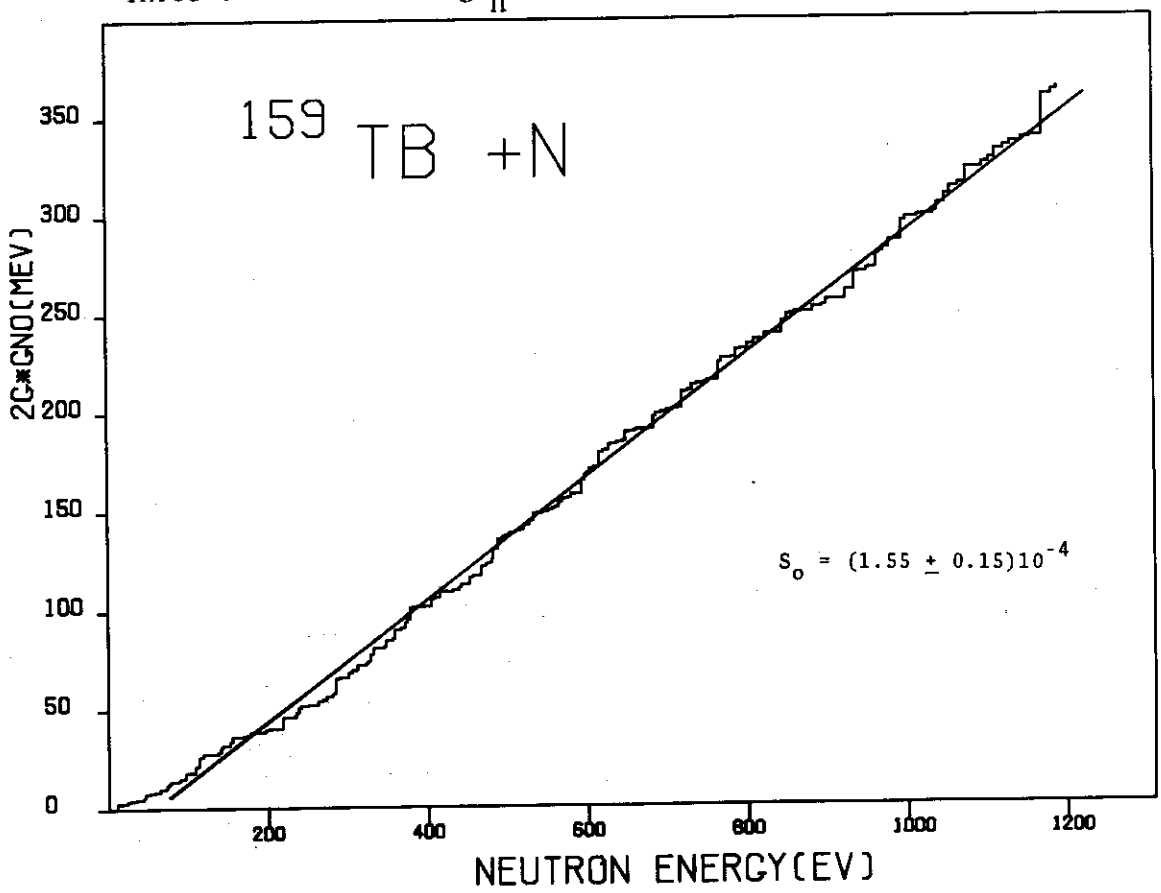

Fig.11 Cumulative value of $2g\Gamma_n^o$ vs. neutron energy up to 1.2 keV.

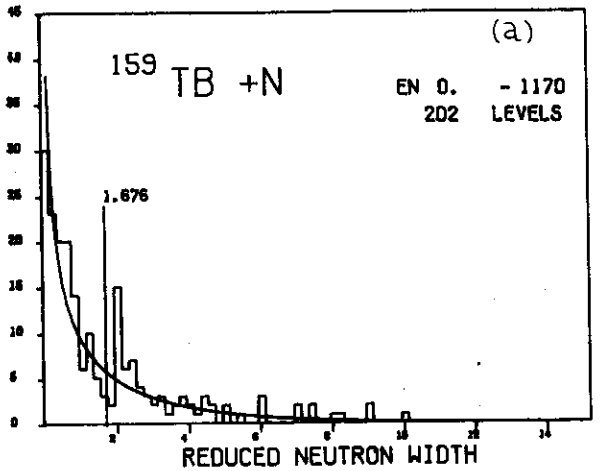

Fig.12a. Reduced neutron width ($2g\Gamma_n^o$) distribution for the level below 1.2 keV. Average value and the Porter-Thomas distribution curve are shown.

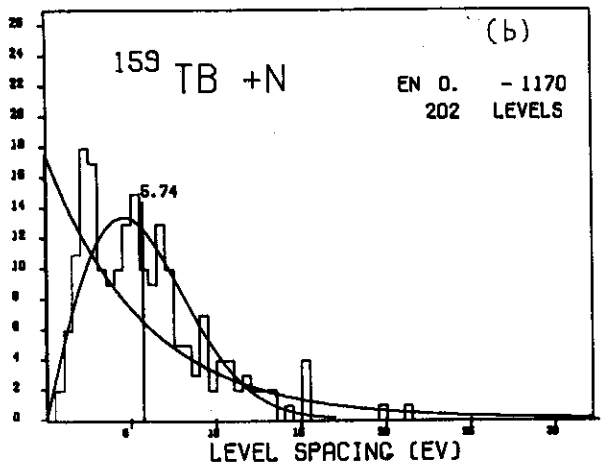

Fig.12b. Spacing distribution between adjacent levels. Average value and the Wigner and Random distributions are also shown.

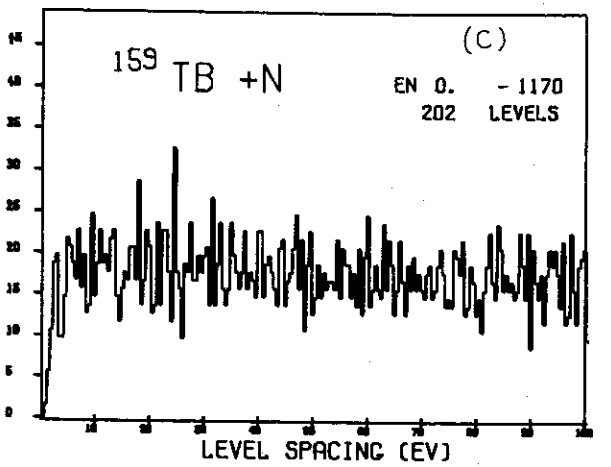

Fig.12c. Spacing distribution between arbitrary two levels.

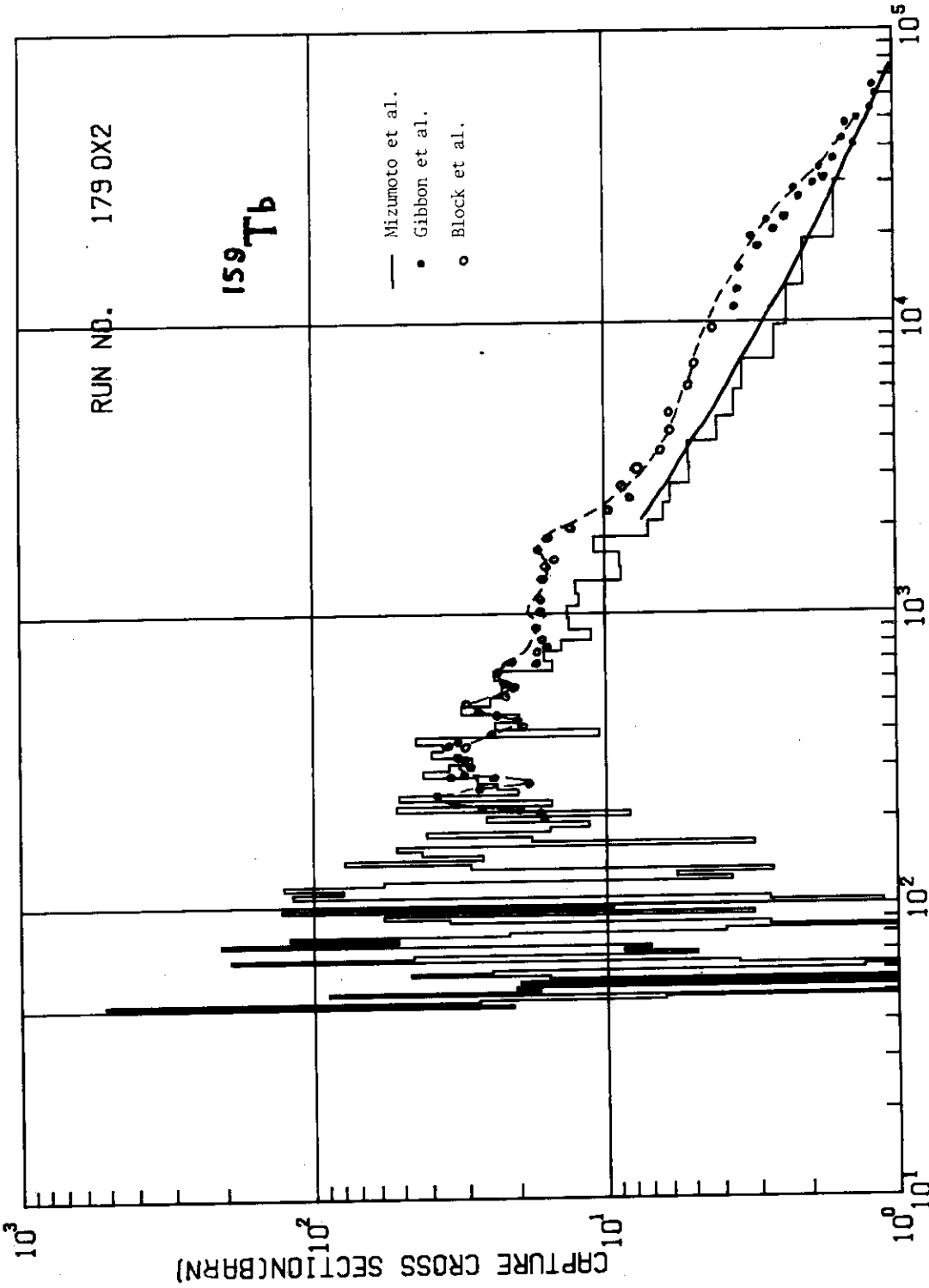

Fig. 13 Average capture cross section up to 30 keV. The values by other authers are also shown.

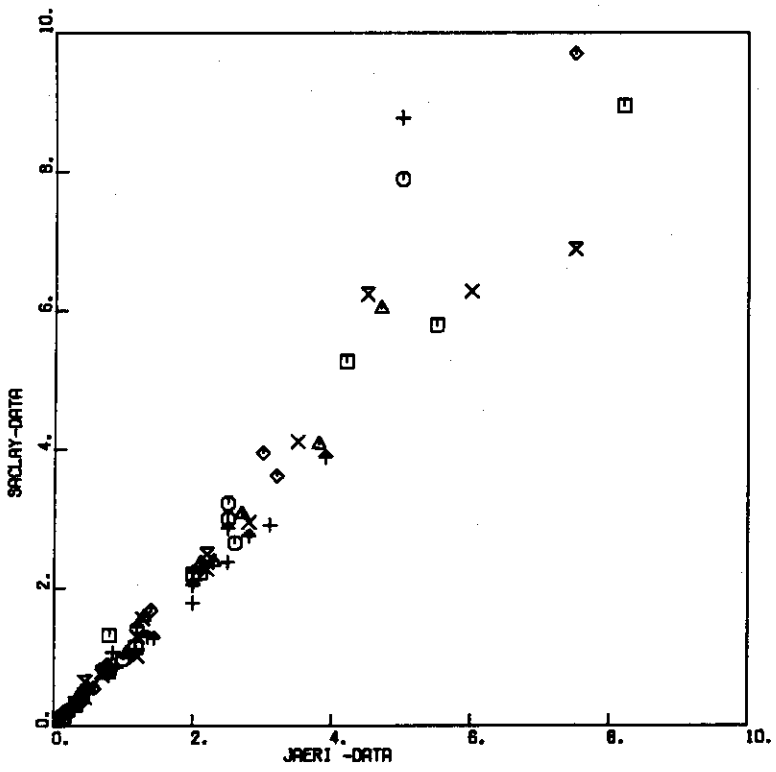

Fig.14a Comparison of JAERI and SACLAY data for each resonances. Plot of $2g\Gamma_n^o$, with ordinate SACLAY values and in abscissa JAERI values.

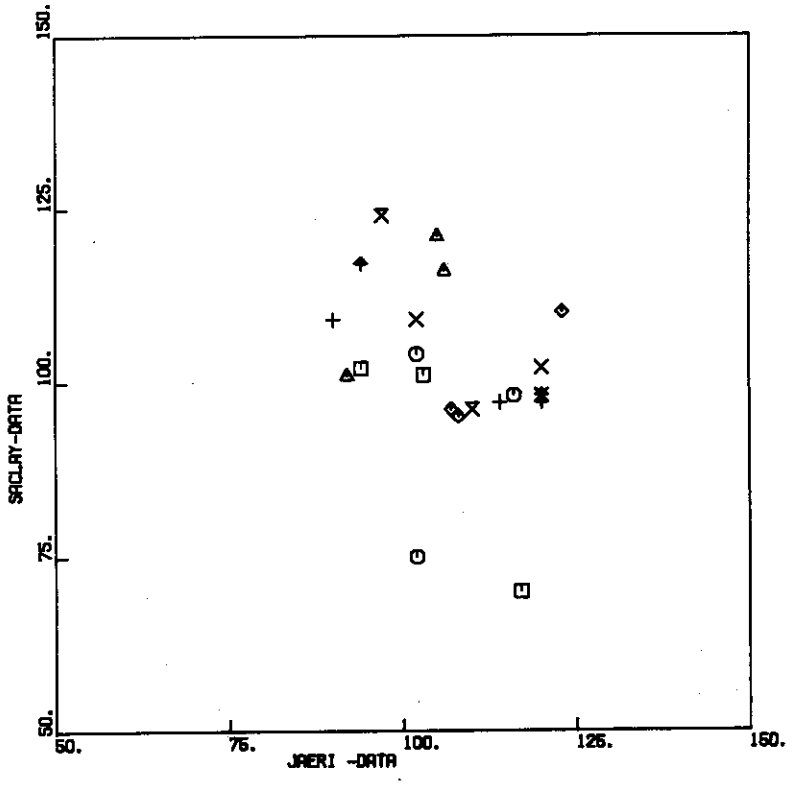

Fig.14b Plot of Γ_γ for each resonance, with ordinate SACLAY values and in abscissa JAERI values.